

This article was downloaded by:

On: 21 January 2011

Access details: *Access Details: Free Access*

Publisher *Taylor & Francis*

Informa Ltd Registered in England and Wales Registered Number: 1072954 Registered office: Mortimer House, 37-41 Mortimer Street, London W1T 3JH, UK



International Journal of Polymer Analysis and Characterization

Publication details, including instructions for authors and subscription information:

<http://www.informaworld.com/smpp/title~content=t713646643>

Simulations of Partitioning in Size Exclusion Chromatography

Peter Cifra^a; Tomá Bleha^a

^a Polymer Institute, Slovak Academy of Sciences, Bratislava, Slovakia

To cite this Article Cifra, Peter and Bleha, Tomá(2001) 'Simulations of Partitioning in Size Exclusion Chromatography', *International Journal of Polymer Analysis and Characterization*, 6: 6, 509 – 520

To link to this Article: DOI: 10.1080/10236660108030866

URL: <http://dx.doi.org/10.1080/10236660108030866>

PLEASE SCROLL DOWN FOR ARTICLE

Full terms and conditions of use: <http://www.informaworld.com/terms-and-conditions-of-access.pdf>

This article may be used for research, teaching and private study purposes. Any substantial or systematic reproduction, re-distribution, re-selling, loan or sub-licensing, systematic supply or distribution in any form to anyone is expressly forbidden.

The publisher does not give any warranty express or implied or make any representation that the contents will be complete or accurate or up to date. The accuracy of any instructions, formulae and drug doses should be independently verified with primary sources. The publisher shall not be liable for any loss, actions, claims, proceedings, demand or costs or damages whatsoever or howsoever caused arising directly or indirectly in connection with or arising out of the use of this material.

Simulations of Partitioning in Size Exclusion Chromatography

Peter Cifra and Tomáš Bleha

Polymer Institute, Slovak Academy of Sciences,
Bratislava, Slovakia

The systematic investigations by Monte Carlo (MC) simulations of parameters involved in partitioning in size exclusion chromatography (SEC) are reported. Specifically, three realistic features involved in the separation mechanism are treated: (a) real chain features as contrast to ideal chain behavior, (b) finite concentration of macromolecules in partitioning, and (c) adsorption of polymer on pore walls. In all cases an enhancement of the partitioning relative to the ideal circumstances was found. The partitioning rules in these cases significantly deviate from the Casassa relation for ideal chains. The factors mentioned affect the shape of the universal calibration dependence and reduce its selectivity. The rationalization of the free energy of confinement in SEC based on a loss of orientational entropy of coil ellipsoids in a pore is suggested.

Keywords: Computer simulations; SEC; Separation mechanism; Universal calibration

INTRODUCTION

The partitioning of macromolecular solutes between small pores and bulk solution underlies various chromatographic and membrane separation processes. This phenomenon is characterized by the partition coefficient K , which is the pore-to-bulk concentration ratio at

Received 29 November 1999; In final form 15 January 2001.

Address correspondence to Tomáš Bleha, Polymer Institute, Slovak Academy of Sciences, 842 36 Bratislava, Slovakia. E-mail: upoltble@savba.sk

Presented at the 13th Bratislava International Conference on Polymers, "Separation and Characterization of Macromolecules," Bratislava, Slovakia, July 4–9, 1999.

equilibrium. The theoretical models of partitioning of flexible macromolecules were recently reviewed^[1]. In earlier treatment the pure steric exclusion of ideal chains in infinitely dilute solutions was addressed and K was expressed^[2,3] as a function of the coil-to-pore size ratio $\lambda = R_g/D_p$, where R_g is the radius of gyration of a chain and D_p is the characteristic dimension of a pore. The coefficient K is related to the free energy of confinement $\Delta A = -kT \ln K$. Since steric interaction between a macromolecule and a pore is dominant separation mechanism in the size exclusion chromatography (SEC), the analytical relations K vs λ due to Casassa^[2,3] (the partitioning rules) are widely used in SEC.

In order to understand the separation and transport of polymers *in real systems*, additional factors, not accounted for in the Casassa treatment, have to be considered. These factors include the finite length of chains and their polydispersity, intrachain excluded volume and quality of solvent, limitations on the chain flexibility, the distribution of pore sizes and shapes, polymer/matrix interaction, solute concentration, etc. The role of some of the mentioned variables in polymer partitioning was already investigated. For example, the analytical approach of Casassa for the ideal chains was extended to include the adsorption of polymers on the pore walls^[4,5]. The effect of the thermodynamic quality of the solvent^[6] and of polymer concentration^[7-9] on the function K vs λ was evaluated by computer simulations.

In this paper we present the results of a systematic study of nonideal polymer partitioning into the large pores by Monte Carlo (MC) simulations. Specifically, three factors relevant to the separation mechanism of SEC were considered: (a) chains with realistic features instead of ideal chains, (b) finite polymer concentration, and (c) adsorption of macromolecules on pore walls. The results show that all above parameters enhance polymer partitioning relative to the ideal situation. Moreover, the latter two factors change the shape of the universal calibration plot and reduce the selectivity of the SEC separation.

SIMULATION MODEL

The simulation procedure was described previously^[10]. Two boxes connected to each other are assumed on a cubic lattice: the box E , representing the exterior (bulk) phase and box I , representing the interior of a slit-like pore. The slit width $D = 2D_p$ is defined as the distance between the lattice layers occupied by the walls and is measured in lattice units. The polymer beads are not allowed to occupy the sites on the walls. Periodic boundary conditions apply with respect to all opposite walls in boxes except the solid walls.

The self-avoiding walks of the variable length N up to 100 beads in chains were generated in two solvent regimes. The athermal model of zero

value of the reduced energy ϵ_S of segment-segment contacts, represented good solvents. The theta chains were generated using the reduced attractive energy^[11] $\epsilon_s = -0.2693$. In some simulations short-range adsorption interaction ϵ_w ($\epsilon_w < 0$) was considered between polymer segments and wall sites separated by one lattice unit. The strength of the reduced attraction energy per segment ϵ_w varied from 0 (pure steric exclusion) to -0.3 , thus covering the region of weakly adsorbed chains.

Chains were equilibrated using the reptation moves and the Metropolis algorithm. The ratio of the volume fractions of a polymer in the interior and exterior boxes at equilibrium ϕ_I/ϕ gave the coefficient K . The exterior concentrations ϕ up to 0.13 were used. The root-mean-square radius of gyration R_g of the free unconfined chains was determined by the standard procedure.

RESULTS AND DISCUSSION

The partitioning rule of Casassa refers to the ideal partitioning of the random-flight chains composed of noninteracting segments. The present simulations extend Casassa's approach by the incorporation of factors from actual chromatographic practice such as real chain features of separated polymers, the finite concentration of macromolecules in a mobile phase, and adsorption of polymer solutes on the column packing. Moreover, good solvents, frequently used as a mobile phase in SEC, demand the consideration of the excluded volume chains instead of ideal chains. In the simulations, the region of the SEC partitioning was addressed, where the pore size is larger than the size of solutes ($\lambda < 1$).

Influence of Real Chain Features

The partitioning coefficient K_0 refers to an "ideal" SEC, based on the pure steric exclusion mechanism at infinite dilution. The properties of real chains are influenced by parameters such as the chain length N , the length of (Kuhn) chain segment b related to the chain flexibility, intramolecular excluded volume, etc. These and similar characteristics of the real chains may affect the SEC partitioning curve K_0 vs λ .

The MC results of partitioning of theta and athermal chains into a slit at infinite dilution are shown in Figure 1. The Casassa ideal chain function in a slit^[2,3], which in the region $\lambda \ll 1$ predicts a linear decrease of K_0 with λ , is also shown in Figure 1 as a reference. The results for both excluded volume chains seem to obey the same dependence of K_0 on λ . Evidently, the effect of the thermodynamic quality of a solvent is entirely suppressed in the representation of the partitioning data by the plot K_0 vs λ , in agreement with previous observation^[6].

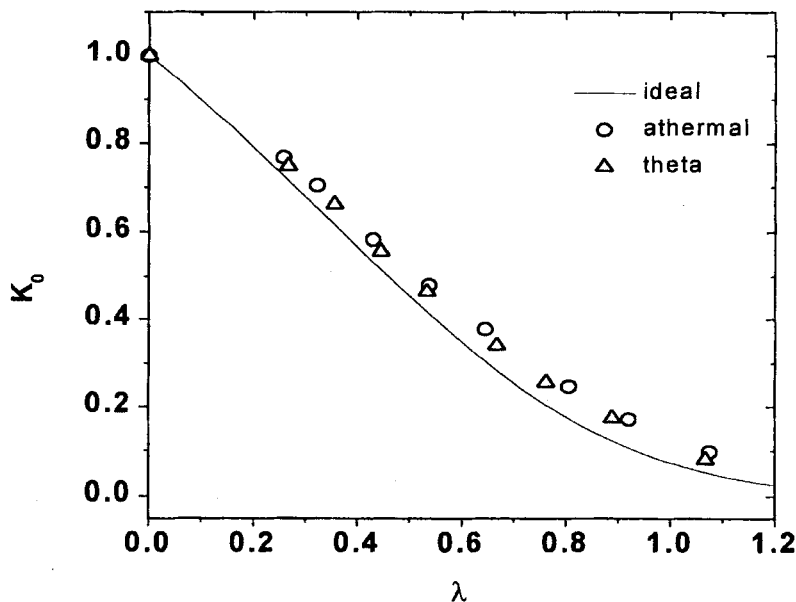


FIGURE 1 Variation of the partition coefficient K with the ratio λ in a slit.

The MC results for both types of real chains are shifted to higher K relative to ideal (Gaussian) chains for a given λ . The same trend was discernible^[1] in our previous treatment^[7,8] of shorter ($N=20-60$) athermal chains. The freely jointed model of ideal chains assumes an infinite number of chain segments with vanishingly small mean length. The enhancement of partitioning of real chains relative to the ideal chains shown in Figure 1 can be attributed both to chain excluded volume and to the finite segment length b (restricted flexibility) in the real chains. A substantial increase of K_0 with the increase of the segment length b was already observed in earlier simulations^[12].

The plot of $\log V_h$ (hydrodynamic volume) versus retention volume V_R , denoted the universal calibration, is frequently used to present the data in SEC. The partition coefficient K is related to V_R by the equation $V_R = V_0 + KV_I$, where V_0 is the volume of the interstitial mobile phase and V_I the volume of the quasi-stationary phase within the pores. The hydrodynamic volume V_h , usually approximated by the product of intrinsic viscosity and molecular weight, is linked up to R_h , the hydrodynamic radius of a macromolecular coil. The radius R_h is closely related to the radius of gyration R_g . For coils $R_h/R_g < 1$, and the exact value of this ratio depends slightly on chain flexibility. Consequently, the term $\log V_h$ is proportional to $3 \log R_g$. Hence, the term $(3 \log R_g + c)$, where c

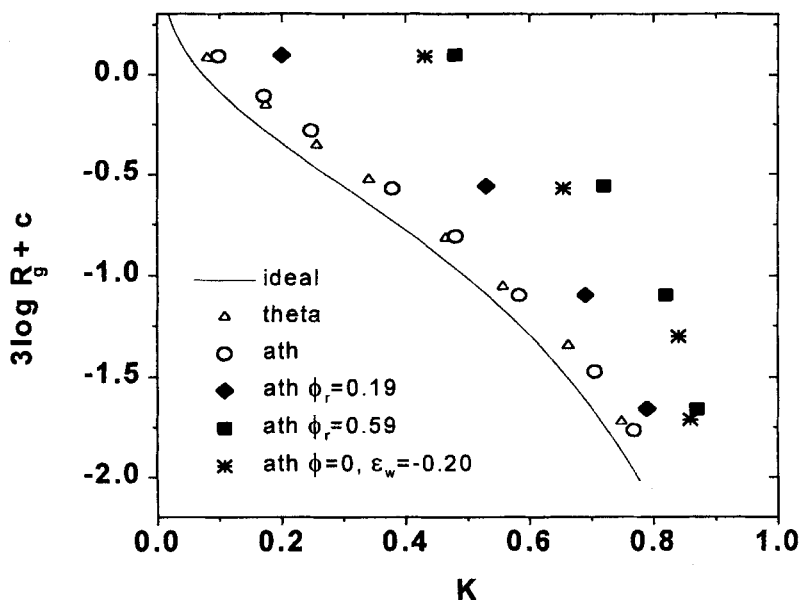


FIGURE 2 The simulation of the universal calibration in a slit.

is a numerical constant, plotted as a function of K , represents a variant of the universal calibration for a given column (with a fixed pore size). It is seen (Figure 2) that in "ideal" SEC, based on pure steric exclusion mechanism, the universal calibration evaluated from simulations of real molecules is shifted to higher K_0 relative to an analogous plot for ideal chains. Apparently, in "ideal" SEC the concept of a universal calibration remains valid for the small differences in the chain excluded volume and/or chain flexibility (Kuhn segment length) between the polymer standard and the investigated polymer. On the contrary, flexible and semiflexible (in which many monomer units form one segment) polymers of the same R_g will exhibit different universal calibrations as demonstrated earlier by experiments and simulations^[13,14].

Steric Partitioning in Dilute Solutions

Measurements of polymer partitioning at static conditions^[15] show that in good solvents the coefficient K increases with bulk concentration ϕ . The results of MC simulation in good (athermal) solvent (Figure 3) confirm that an increase of the bulk concentration enhances the penetration of molecules into a pore. In the region of very dilute solution the increase

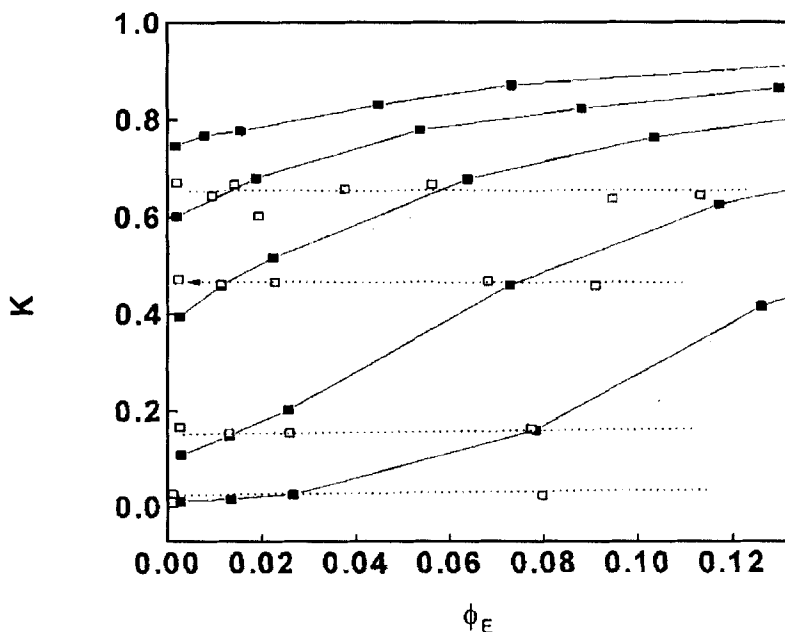


FIGURE 3 The concentration effect on the partition coefficient K . Athermal chains (full lines) for $\lambda = 0.28; 0.43; 0.65; 1.08; 1.61$ (from above), the theta chains (dotted) for $\lambda = 0.36, 0.53, 0.89, 1.33$.

of K is approximately linear in agreement with our previous simulations of shorter chains^[7,8]. The concentrations in Figure 3 cover the regime of a dilute solution, below the onset of coil overlap at the critical concentration $\phi^* = N/(\sqrt{2}R_g)^3 = 0.132$. Similar simulations for athermal chains were reported^[9] in a slightly different range of pore widths.

In striking contrast to the good solvent, the negligible concentration effect on K was found from simulations in the theta solvent (Figure 3). Evidently, the steric partitioning in the dilute solutions is exceedingly affected by the solvent quality. So far no measurements of the static partitioning in theta solvents were reported in the literature. However, the concentration dependence of K can be inferred from the dynamic partitioning in SEC, specifically, from the shift of the peak elution volume V_R with the concentration c of the injected volume. Similarly to the data in Figure 3, the large concentration effect on V_R was observed in good solvents as eluents and a negligible one was found in the theta eluents^[16,17]. From the measurements of the concentration effect in SEC in eluents of variable thermodynamic quality for injected polymers, a strong correlation was established^[17,18] between the rate of increase of K

with c and the product A_2M , where A_2 is the second osmotic virial coefficient. The simulation results in Figure 3 lend support to this correlation and confirm a common nature of the concentration effect in the static partitioning and in SEC. In both cases this phenomenon results from deviations from ideality in the bulk (external) solution that can be quantified by the term A_2M . Using the concept of repulsive interactions between macromolecules, microscopic models^[1,19] of the concentration effect were developed. However, hitherto the models were applied only to the partitioning in good solvents. For example, the deviation of K from its value in very dilute solutions K_0 was related^[1] to the osmotic pressure in the bulk solution of concentration ϕ . The osmotic pressure drives the macromolecules (preferably shorter ones) into the pore.

The finite concentrations in good (athermal) solvent affect the universal calibration in the way illustrated in Figure 2 for two values of $\phi_r = \phi/\phi^*$, 0.19, and 0.59. It is seen that enhanced concentrations further amplify the shift of the universal calibration to higher values of K . Moreover, in this case, the shape of the plot is also changed. The selectivity of separation is reduced; the resolution power of SEC diminishes at finite concentration.

Partitioning by Steric Exclusion and Adsorption in Very Dilute Solutions

The adsorption of solute on the solid matrix such as column packing is frequently experienced in the partitioning of macromolecules. The mixed mode (steric exclusion/adsorption) mechanism of partitioning of real chains in good solvents at infinite dilution was simulated by an interplay of two potentials: (a) hard core repulsion of chain segments on the lattice ($\epsilon_S = 0$) and (b) attraction between slit walls and the first-neighbor chain segments of the strength ϵ_w . Variations of the reduced adsorption energy can be interchanged with the variations of the temperature.

The gradual change of the shape of the partitioning curve K vs λ in slit with increasing attraction ϵ_w is shown in Figure 4 for the athermal chains of lengths of 100 segments. The curve for $\epsilon_w = 0$ corresponds to pure steric exclusion. The partitioning curves become more flat for $-\epsilon_w > 0$ and are shifted to higher λ . Thus, the sorption effects can be seen as an apparent widening of pores or shortening of the chain length. The presence of attractive polymer-pore interaction obviously affects the universal calibration, and its slope (selectivity) is reduced by increased attraction (Figure 2). In this respect the influence of pore attraction is comparable to the one of concentration.

The differences in the adsorption energy of solutes are responsible for their separation in liquid adsorption chromatography. In real SEC of macromolecules on porous packing, the combined effect of steric

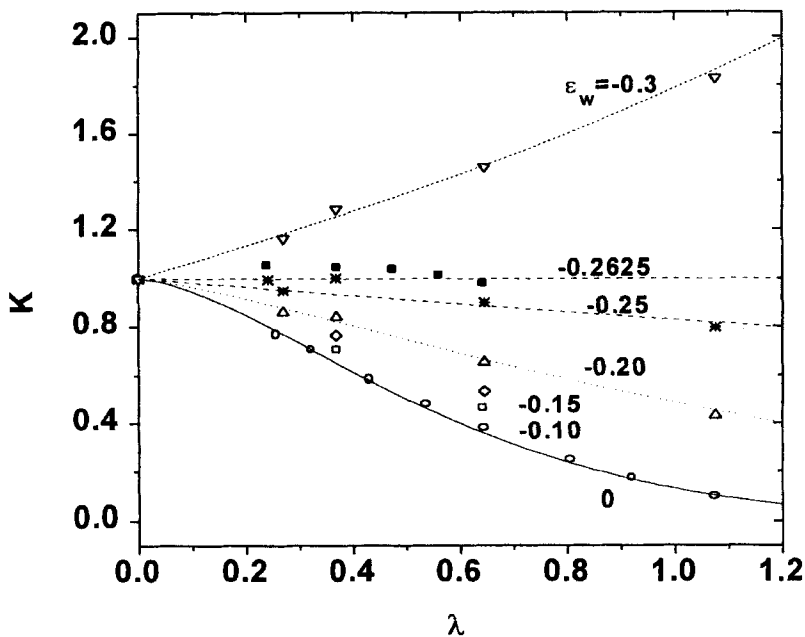


FIGURE 4 The influence of the attraction strength ϵ_w on the shape of the partitioning curve.

exclusion and adsorption mechanisms is frequently operative. As shown in Figure 4, the different regimes of the steric exclusion/adsorption equilibrium in chromatography of real macromolecules can be reproduced by the variation of ϵ_w in simulations, including the region of the critical chromatography around $K=1$. This region, where attractive interaction of walls should counterbalance the polymer-pore exclusion, is of particular interest for the theory and chromatographic practice. Experimental results^[20] suggest that the critical chromatography can exploit in separation the small differences in the chemical composition of macromolecules.

The simulation results for the excluded volume chains can be ascertained with the mixed-mode partitioning theory of Skvortsov and Gorbunov^[4,5] for ideal chains. In their theory, the partition coefficient K is expressed as a function of three parameters: R_g , D_p , and H . The correlation length of adsorption, H , is related to the attraction strength by the proportionality $H \approx b/(\epsilon_w^* - \epsilon_w)$ where ϵ_w^* corresponds to the critical point of adsorption. The theory of ideal chains predicts^[4,5,21] that in the compensation point $K=1$ the free energy of a chain in a pore and in bulk is equal, and thus the partition coefficient K is independent of the

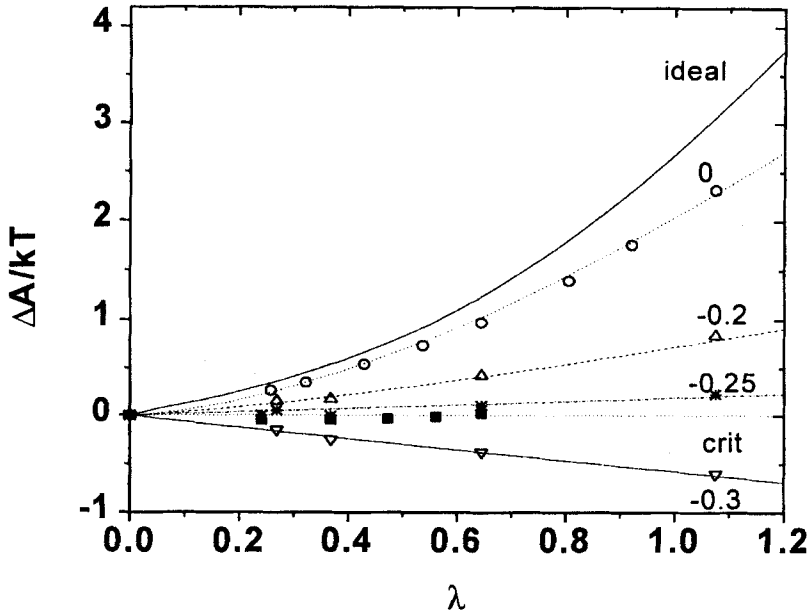


FIGURE 5 The influence of the attraction strength ε_w on the free energy of confinement.

molecular mass M of the solute. The results for real chains of the length $N=100$ show (Figure 4) that the steric exclusion and adsorption effects fully compensate at $\varepsilon_w^* = -0.2625$. The detailed study of the compensation region^[10] revealed that the attraction strength at the compensation point, ε_w^* , in the excluded volume chains depends on their length N . In other words, the simulations of real chains^[10] predict that the compensation point in the critical chromatography with good solvents should change with M in the narrow interval of the adsorption strengths.

The steric exclusion/adsorption partitioning data can be used to plot the free energy of confinement $\Delta A/kT = -\ln K$ as a function of the coil-to-pore size ratio λ (Figure 5). The free energy penalty due to confinement is maximum at pure steric exclusion. An increase in the attraction strength reduces the disadvantage of the confinement. Interestingly, at the attraction strengths higher than critical, for example at $\varepsilon_w = -0.3$, a molecule in the pore becomes more stabilized than a molecule in the bulk phase.

The Decomposition of K

The effective partition coefficient K of macromolecules in SEC at real conditions is frequently expressed by different combinations of the term K_0 that refers to purely steric exclusion at infinite dilution and of some "corrections" K_{sec} due to secondary separation mechanisms. The latter term may include the contributions due to polymer adsorption, finite solute concentration, liquid-liquid partition, electrostatic interaction, etc. Sometimes, a simple summation of these terms is assumed, $K = K_0 + K_{\text{sec}}$. For example, the concentration effect on K , such as shown in Figure 3, can formally be expressed as a sum $K = K_0 + K_\phi$, where K_ϕ is the finite concentration term. In a similar vein, $K = K_0 + K_e$ applies to the steric exclusion/adsorption partitioning at infinite dilution, where K_e is the adsorption term. Such a summation of individual terms in the coefficient K is useful^[22,23] in the elucidation of the contributions to the separation mechanisms in SEC. For example the modification of the partitioning curves K vs λ shown in Figure 4 can be qualitatively explained by using the latter equation.

In an alternative procedure, the free energy terms operative in the real SEC, instead of contributions to the coefficient K , are summed. The pure steric free energy of confinement ΔA_0 at infinite dilution is supplemented by the appropriate free energy term(s) of the secondary mechanism(s), $\Delta A = \Delta A_0 + \Delta A_{\text{sec}}^*$. This notion of the free energy additivity is readily understandable for the steric exclusion/adsorption mechanism from the plot in Figure 5. However, in this procedure the overall partitioning coefficient K is given by the product^[24] of the terms K_0 and $K_{\text{sec}}^* = \exp(-\Delta A_{\text{sec}}^*/kT)$, i.e., $K = K_0 K_{\text{sec}}^*$. In principle both procedures are equivalent; however, one should bear in mind that the secondary "correction" terms in both procedures are different, $K_{\text{sec}} \neq K_{\text{sec}}^*$.

The Free Energy of Confinement in SEC

The free energy of confinement ΔA of a macromolecule in a pore is intimately connected with the changes in the dimensions and in the shape of flexible macromolecules at confinement. These changes can be inferred from simulations^[25,26] of molecules confined in pores of a regular geometry. From information on the mean-square end-to-end distance $\langle R^2 \rangle$ and on the radius of gyration R_g , as well as on their components in the parallel and perpendicular directions to the pore walls, as a function of the slit width D , the following picture ensued from simulations: In an unconfined situation, single macromolecules, shaped as prolate ellipsoids, are randomly oriented. At weak confinement in a slit, the cigar-shaped molecules remain essentially undeformed, just align along the pore walls.

Further on, at moderate confinements, molecules become compressed along all three axes. Finally, at strong confinements (narrow slits) the shape of molecules resembles the quasi-two-dimensional disks.

Since SEC operates in the range of weak confinement (λ is much below 1), the changes in the inherent shape of molecular ellipsoids during separation should be minor. Thus, the steric free energy of confinement ΔA_0 at infinite dilution can be interpreted^[26] mostly as the result of the loss of orientational entropy due to the alignment of ellipsoid molecules along the pore walls. A number of orientations of a coil ellipsoid are not allowed due to steric exclusion of pore walls. In contrast, the traditional explanation of the mechanism of SEC emphasizes a loss of conformational entropy since conformations crossing the pore walls are rejected. However, the elimination of conformations crossing the walls actually corresponds to the effective modification of the coil shape. The simulations^[25,26] indicate that the "true" deformation of an intrinsic shape of coil ellipsoids should be of secondary importance for the pore size in SEC region. The coil deformation mechanism should dominate at strong confinements, resulting in the flattening of coil ellipsoids and ultimately in the formation of nearly two-dimensional "pancakes".

An inclusion of the weak pore attraction produced no substantial changes in the size and shape of confined macromolecules^[10]. Accordingly, also in this case, the entropy term should originate mainly from the alignment of ellipsoid molecules along the pore walls. However, the enthalpy term due to attractive interaction contributes to the free energy of confinement ΔA in this case. Since $\Delta H < 0$, the enthalpy term partially reduces the free energy penalty (Figure 5). At the compensation point, the loss of orientational entropy is fully balanced by the (adsorption) enthalpy of confinement. At the attraction strengths higher than critical, the term ΔH outweighs the entropy loss of a chain in a slit and ΔA becomes negative.

CONCLUSIONS

The presented results show that Monte Carlo simulations are well suited to investigate all the primary factors in the partitioning of macromolecules at conditions relevant to SEC practice. The simulations allow separate consideration of individual factors, which are usually coupled in experiments. The partitioning properties of flexible chains were ascertained in three cases studied: (a) partitioning of real chains (as contrasts to ideal chains), (b) the finite polymer concentration in partitioning, and (c) adsorption of molecules on pore walls. The partitioning rules significantly deviate from the Casassa relation for ideal chains. In all cases an enhancement of the partitioning relative to the ideal circumstances

was observed. The factors mentioned should affect the shape of the universal calibration and reduce the selectivity of the SEC separation. Nature of the free energy of confinement in SEC was discussed, and the interpretation based on the loss of the orientational entropy of coil ellipsoids in a pore was advanced.

ACKNOWLEDGMENTS

The research was supported in part by the Grant Agency for Science (VEGA), grants No. 2/7056/20 and 2/7076/20. The use of computer resources of the Computing Centre of SAS is gratefully acknowledged.

REFERENCES

- [1] I. Teraoka (1996). *Prog. Polym. Sci.* **21**, 89.
- [2] E. F. Casassa (1967). *J. Polym. Sci., Polym. Lett. Ed.* **5**, 773.
- [3] E. F. Casassa and Y. Tagami (1969). *Macromolecules* **2**, 14.
- [4] A. A. Gorbunov and A. M. Skvortsov (1995). *Adv. Colloid Interface Sci* **62**, 31.
- [5] A. M. Skvortsov and A. A. Gorbunov (1986). *J. Chromatogr.* **358**, 77.
- [6] P. Cifra, T. Bleha, and A. Romanov (1988). *Polymer* **29**, 1664.
- [7] P. Cifra, T. Bleha, and A. Romanov (1988). *Macromol. Chem. Rapid Commun.* **9**, 335.
- [8] T. Bleha, P. Cifra, and F. E. Karasz (1990). *Polymer* **31**, 1321.
- [9] Y. Wang and I. Teraoka (1997). *Macromolecules* **30**, 8473.
- [10] P. Cifra and T. Bleha (2000). *Polymer* **41**, 1003.
- [11] W. Bruns (1984). *Macromolecules* **17**, 2826.
- [12] M. G. Davidson, U. W. Suter, and W. M. Deen (1987). *Macromolecules* **20**, 1141.
- [13] P. L. Dubin and J. M. Principi (1989). *Macromolecules* **22**, 1891.
- [14] Ch. Degoulet, J.-P. Busnel, and J.-F. Tassin (1994). *Polymer* **35**, 1957.
- [15] I. Teraoka (1996). *Macromolecules* **29**, 2430.
- [16] D. Berek, D. Bakoš, T. Bleha, and L. Šoltés (1975). *Makromol. Chem.* **176**, 391.
- [17] T. Bleha, T. Spychaj, R. Vondra, and D. Berek (1983). *J. Polym. Sci. Polym. Phys. Ed.* **21**, 1903.
- [18] T. Bleha, J. Mlýnek, and D. Berek (1980). *Polymer*, **21**, 798.
- [19] A. P. Thompson and E. D. Glandt (1996). *Macromolecules*, **29**, 4314.
- [20] D. Berek (1996). *Macromol. Symp.* **110**, 33.
- [21] C. M. Guttman, E. A. DiMarzio, and J. F. Douglas (1996). *Macromolecules* **29**, 5723.
- [22] D. Bakoš, T. Bleha, A. Ozimá, and D. Berek (1979). *J. Appl. Polym. Sci.* **23**, 2233.
- [23] A. A. Gorbunov and A. M. Skvortsov (1986). *Vysokomol. Soed. A* **28**, 2453.
- [24] J. V. Dawkins and M. Hemming (1975). *Makromol. Chem.* **176**, 1795.
- [25] J. H. van Vliet, M. C. Luyten, and G. ten Brinke (1992). *Macromolecules* **25**, 3802.
- [26] P. Cifra and T. Bleha (1999). *Macromol. Theory Simul.* **8**, 603.